75 MW few-cycle mid-infrared pulses from a collinear apodized APPLN-based OPCPA

C. Heese,[1] C. R. Phillips, [2,*] B. W. Mayer,[1] L. Gallmann,[1] M. M. Fejer,[2] and U. Keller[1]

[1]*Department of Physics, Institute of Quantum Electronics, ETH Zurich, 8093 Zurich, Switzerland*
[2]*Edward L. Ginzton Laboratory, Stanford University, Stanford, California 94305,USA*
[*]*cphillips@phys.ethz.ch*

Abstract: We present an ultra-broadband optical parametric chirped-pulse amplification (OPCPA) system operating at 3.4 μm center wavelength with a peak power of 75 MW. The OPCPA system is split into a pre- and a power-amplifier stage. Both stages are based on apodized aperiodically poled MgO:$LiNbO_3$ (APPLN). The collinear mixing configuration allows us to manipulate the spectral phase of the output mid-infrared pulses by sending the near-infrared seed pulses through a pulse shaper. The system delivers clean 75-fs pulses with record-high 700 mW average power, corresponding to 7 μJ of pulse energy at a repetition rate of 100 kHz.

OCIS codes: (140.7090) Ultrafast lasers; (190.4970) Parametric oscillators and amplifiers; (140.3580) Lasers, solid-state.

References and links

1. A. D. Shiner, C. Trallero-Herrero, N. Kajumba, H. C. Bandulet, D. Comtois, F. Légaré, M. Giguère, J. C. Kieffer, P. B. Corkum, and D. M. Villeneuve, "Wavelength Scaling of High Harmonic Generation Efficiency," Phys. Rev. Lett. **103**(7), 073902 (2009).
2. P. Colosimo, G. Doumy, C. I. Blaga, J. Wheeler, C. Hauri, F. Catoire, J. Tate, R. Chirla, A. M. March, G. G. Paulus, H. G. Muller, P. Agostini, and L. F. DiMauro, "Scaling strong-field interactions towards the classical limit," Nat. Phys. **4**(5), 386–389 (2008).
3. K. D. Schultz, C. I. Blaga, R. Chirla, P. Colosimo, J. Cryan, A. M. March, C. Roedig, E. Sistrunk, J. Tate, J. Wheeler, P. Agostini, and L. F. DiMauro, "Strong field physics with long wavelength lasers," J. Mod. Opt. **54**(7), 1075–1085 (2007).
4. J. Tate, T. Auguste, H. G. Muller, P. Salières, P. Agostini, and L. F. DiMauro, "Scaling of Wave-Packet Dynamics in an Intense Midinfrared Field," Phys. Rev. Lett. **98**(1), 013901 (2007).
5. P. B. Corkum, "Plasma perspective on strong field multiphoton ionization," Phys. Rev. Lett. **71**(13), 1994–1997 (1993).
6. S. Baker, J. S. Robinson, C. A. Haworth, H. Teng, R. A. Smith, C. C. Chirilă, M. Lein, J. W. G. Tisch, and J. P. Marangos, "Probing Proton Dynamics in Molecules on an Attosecond Time Scale," Science **312**(5772), 424–427 (2006).
7. C. Vozzi, R. Torres, M. Negro, L. Brugnera, T. Siegel, C. Altucci, R. Velotta, F. Frassetto, L. Poletto, P. Villoresi, S. De Silvestri, S. Stagira, and J. P. Marangos, "High harmonic generation spectroscopy of hydrocarbons," Appl. Phys. Lett. **97**(24), 241103 (2010).
8. T. Fuji, N. Ishii, C. Y. Teisset, X. Gu, T. Metzger, A. Baltuška, N. Forget, D. Kaplan, A. Galvanauskas, and F. Krausz, "Parametric amplification of few-cycle carrier-envelope phase-stable pulses at 2.1 microm," Opt. Lett. **31**(8), 1103–1105 (2006).
9. G. Andriukaitis, T. Balčiūnas, S. Ališauskas, A. Pugžlys, A. Baltuška, T. Popmintchev, M.-C. Chen, M. M. Murnane, and H. C. Kapteyn, "90 GW peak power few-cycle mid-infrared pulses from an optical parametric amplifier," Opt. Lett. **36**(15), 2755–2757 (2011).
10. T. Wilhelm, J. Piel, and E. Riedle, "Sub-20-fs pulses tunable across the visible from a blue-pumped single-pass noncollinear parametric converter," Opt. Lett. **22**(19), 1494–1496 (1997).
11. A. Shirakawa, I. Sakane, M. Takasaka, and T. Kobayashi, "Sub-5-fs visible pulse generation by pulse-front-matched noncollinear optical parametric amplification," Appl. Phys. Lett. **74**(16), 2268–2270 (1999).
12. M. Ghotbi, M. Ebrahim-Zadeh, V. Petrov, P. Tzankov, and F. Noack, "Efficient 1 kHz femtosecond optical parametric amplification in BiB3O6 pumped at 800 nm," Opt. Express **14**(22), 10621–10626 (2006).
13. C. J. Fecko, J. J. Loparo, and A. Tokmakoff, "Generation of 45 femtosecond pulses at 3 μm with a KNbO3 optical parametric amplifier," Opt. Commun. **241**(4-6), 521–528 (2004).
14. G. M. Gale, G. Gallot, F. Hache, and R. Sander, "Generation of intense highly coherent femtosecond pulses in the mid infrared," Opt. Lett. **22**(16), 1253–1255 (1997).

#176309 - $15.00 USD Received 18 Sep 2012; revised 2 Nov 2012; accepted 8 Nov 2012; published 14 Nov 2012

15. U. Emmerichs, S. Woutersen, and H. J. Bakker, "Generation of intense femtosecond optical pulses near 3 μm with a kilohertz repetition rate," J. Opt. Soc. Am. B **14**(6), 1480–1483 (1997).
16. F. Tauser, F. Adler, and A. Leitenstorfer, "Widely tunable sub-30-fs pulses from a compact erbium-doped fiber source," Opt. Lett. **29**(5), 516–518 (2004).
17. C. Erny, C. Heese, M. Haag, L. Gallmann, and U. Keller, "High-repetition-rate optical parametric chirped-pulse amplifier producing 1-microJ, sub-100-fs pulses in the mid-infrared," Opt. Express **17**(3), 1340–1345 (2009).
18. O. Chalus, P. K. Bates, M. Smolarski, and J. Biegert, "Mid-IR short-pulse OPCPA with micro-Joule energy at 100kHz," Opt. Express **17**(5), 3587–3594 (2009).
19. C. Heese, C. R. Phillips, L. Gallmann, M. M. Fejer, and U. Keller, "Ultrabroadband, highly flexible amplifier for ultrashort midinfrared laser pulses based on aperiodically poled Mg:$LiNbO_3$," Opt. Lett. **35**(14), 2340–2342 (2010).
20. M. Bradler, C. Homann, and E. Riedle, "Mid-IR femtosecond pulse generation on the microjoule level up to 5 μm at high repetition rates," Opt. Lett. **36**(21), 4212–4214 (2011).
21. G. Cerullo and S. Silvestri, "Ultrafast optical parametric amplifiers," Rev. Sci. Instrum. **74**(1), 1–17 (2003).
22. S. Witte and K. S. E. Eikema, "Ultrafast Optical Parametric Chirped-Pulse Amplification," IEEE J. Quantum Electron. **18**(1), 296–307 (2012).
23. T. Sudmeyer, S. V. Marchese, S. Hashimoto, C. R. E. Baer, G. Gingras, B. Witzel, and U. Keller, "Femtosecond laser oscillators for high-field science," Nat. Photonics **2**(10), 599–604 (2008).
24. C. R. E. Baer, O. H. Heckl, C. J. Saraceno, C. Schriber, C. Kränkel, T. Südmeyer, and U. Keller, "Frontiers in passively mode-locked high-power thin disk laser oscillators," Opt. Express **20**(7), 7054–7065 (2012).
25. C. Heese, A. E. Oehler, L. Gallmann, and U. Keller, "High-energy picosecond Nd:YVO4 slab amplifier for OPCPA pumping," Appl. Phys. B **103**(1), 5–8 (2011).
26. A. Dubietis, G. Jonusauskas, and A. Piskarskas, "Powerful femtosecond pulse generation by chirped and strechted pulse parametric amplification in BBO crystal," Opt. Commun. **88**(4-6), 437–440 (1992).
27. C. Erny, L. Gallmann, and U. Keller, "High-repetition-rate femtosecond optical parametric chirped-pulse amplifier in the mid-infrared," Appl. Phys. B **96**(2-3), 257–269 (2009).
28. G. Imeshev, M. M. Fejer, A. Galvanauskas, and D. Harter, "Pulse shaping by difference-frequency mixing with quasi-phase-matching gratings," J. Opt. Soc. Am. B **18**(4), 534–539 (2001).
29. K. Mizuuchi, K. Yamamoto, M. Kato, and H. Sato, "Broadening of the phase-matching bandwidth in quasi-phase-matched second-harmonic generation," IEEE J. Quantum Electron. **30**(7), 1596–1604 (1994).
30. U. Kornaszewski, M. Kohler, U. K. Sapaev, and D. T. Reid, "Designer femtosecond pulse shaping using grating-engineered quasi-phase-matching in lithium niobate," Opt. Lett. **33**(4), 378–380 (2008).
31. M. Charbonneau-Lefort, B. Afeyan, and M. M. Fejer, "Optical parametric amplifiers using chirped quasi-phase-matching gratings I: practical design formulas," J. Opt. Soc. Am. B **25**(4), 463–480 (2008).
32. M. Charbonneau-Lefort, M. M. Fejer, and B. Afeyan, "Tandem chirped quasi-phase-matching grating optical parametric amplifier design for simultaneous group delay and gain control," Opt. Lett. **30**(6), 634–636 (2005).
33. M. Charbonneau-Lefort, B. Afeyan, and M. M. Fejer, "Competing collinear and noncollinear interactions in chirped quasi-phase-matched optical parametric amplifiers," J. Opt. Soc. Am. B **25**(9), 1402–1413 (2008).
34. C. R. Phillips and M. M. Fejer, "Efficiency and phase of optical parametric amplification in chirped quasi-phase-matched gratings," Opt. Lett. **35**(18), 3093–3095 (2010).
35. C. Erny, K. Moutzouris, J. Biegert, D. Kühlke, F. Adler, A. Leitenstorfer, and U. Keller, "Mid-infrared difference-frequency generation of ultrashort pulses tunable between 3.2 and 4.8 microm from a compact fiber source," Opt. Lett. **32**(9), 1138–1140 (2007).
36. C. Heese, C. R. Phillips, L. Gallmann, M. M. Fejer, and U. Keller, "Role of apodization in optical parametric amplifiers based on aperiodic quasi-phasematching gratings," Opt. Express **20**(16), 18066–18071 (2012).
37. K. W. DeLong, R. Trebino, J. Hunter, and W. E. White, "Frequency-resolved optical gating with the use of second-harmonic generation," J. Opt. Soc. Am. B **11**(11), 2206–2215 (1994).
38. C. Conti, S. Trillo, P. Di Trapani, J. Kilius, A. Bramati, S. Minardi, W. Chinaglia, and G. Valiulis, "Effective lensing effects in parametric frequency conversion," J. Opt. Soc. Amer. B **19**(4), 852 (2002).
39. J. Huang, X. P. Xie, C. Langrock, R. V. Roussev, D. S. Hum, and M. M. Fejer, "Amplitude modulation and apodization of quasi-phase-matched interactions," Opt. Lett. **31**(5), 604–606 (2006).
40. G. Stobrawa, M. Hacker, T. Feurer, D. Zeidler, M. Motzkus, and F. Reichel, "A new high-resolution femtosecond pulse shaper," Appl. Phys. B **72**(5), 627–630 (2001).

1. Introduction

Mid-infrared (MIR) pulses are of great interest for strong-field experiments, offering a possibility to study the wavelength scaling of light-matter interaction in the non-perturbative regime [1–5]. For instance, with high harmonic generation (HHG), electrons are accelerated in the electric field of one half-cycle of the laser pulse before recollision with the atom [5]. With a long wavelength, for example in the mid-infrared (MIR), acceleration takes place over a longer time interval and results in higher recollision energies at a given optical intensity.

#176309 - $15.00 USD Received 18 Sep 2012; revised 2 Nov 2012; accepted 8 Nov 2012; published 14 Nov 2012

This single aspect already illustrates the intrinsic difference between long- and short-wavelength laser-matter interactions.

A direct application of wavelength scaling in a strong-field process can be found in HHG spectroscopy [6] The measured HHG spectra can be used to derive information about electron or proton dynamics on the attosecond timescale. One difficulty for the extension of this technique to larger and more relevant molecules is the low ionization potential I_p usually found in these systems. At short optical wavelengths, saturation effects of the ionization process constrain this technique to the investigation of molecules with high I_p. This constraint can be overcome by the use of MIR laser pulses, which should enable the study of a much wider range of molecules, in particular biomolecules [7].

For efficient HHG there are constraints on both the peak intensity and total energy of the laser (as well as other system parameters). In order to make high signal-to-noise (SNR) measurements with the generated photons, it is therefore useful to move to higher repetition rates (e.g. 100 kHz) than are used in conventional chirped pulse amplification (CPA) and optical parametric CPA (OPCPA) systems, which usually operate at ≤1 kHz [8–20]. High repetition rates also enable the measurement of fast-degrading samples.

Generating the required high-intensity ultrashort pulses in the MIR is challenging due to the lack of suitable broadband gain media. OPCPA is a promising approach [21, 22], but there is a limited selection of suitable nonlinear crystals for MIR operation. Furthermore, operating an OPCPA system at high-repetition rate places stringent requirements on both the peak and average power of the pump (tens of MW and tens of W, respectively), while still requiring high stability and good beam/pulse quality. At present, the most promising pump lasers for meeting these requirements are mode-locked 1-μm diode-pumped solid-state lasers [23–25]. Developing an approach to broadband MIR OPCPA that is compatible with these lasers is therefore of great importance for the HHG applications described above.

Since the first demonstration of OPCPA [26], several approaches to obtain broad bandwidths have been explored. One way to obtain broadband OPA is to operate at wavelength- and polarization-degeneracy. For example, in Ref [8], 400-μJ, 2.1-μm, 20-fs pulses were obtained from a 1-kHz OPCPA system. However, degenerate operation constrains the wavelengths involved, limiting the range of HHG pump wavelengths that can be studied. Broadband operation can also be obtained by noncollinear OPA (NOPA) [10], but there are few suitable nonlinear crystals available in the MIR, the generated idler is spatially and angularly dispersed, and such schemes can also have the drawback of quite high experimental complexity.

If a sufficiently short signal-idler coupling distance (i.e. a high gain rate) can be obtained, broad bandwidths are possible with non-degenerate collinear OPCPA. Such high gain rates are obtained with periodically poled MgO:$LiNbO_3$. For example, in Ref [17], 1-μJ, 3.6-μm, <100-fs pulses were obtained at 100 kHz. However, the bandwidth possible with this approach is limited by the damage threshold of the crystal [27].

With the high degree of engineerability supported by quasi-phasematching (QPM) [28–30], this bandwidth limitation can be overcome while still maintaining a collinear and non-degenerate interaction. In Refs [31–34], a new approach to OPCPA based on aperiodic (chirped) QPM gratings was proposed. In this approach, there is essentially no intrinsic limit on the optical bandwidth, since a very wide range of QPM periods and crystal lengths can be reliably (lithographically) fabricated, thereby phasematching all frequencies of interest. Therefore, it is possible to utilize power-scalable 1-μm pump lasers without compromising the bandwidth of the OPA process. Additionally, the QPM grating can be engineered to tailor the spectral gain and phase over a large bandwidth [32], and high conversion efficiency is possible via adiabatic frequency conversion [34].

In Ref [19], we demonstrated the first OPCPA system based on this technique, using aperiodically poled MgO:$LiNbO_3$ (APPLN) to generate 1.5-μJ, 3.4-μm, 75-fs pulses at 100 kHz, with seed-limited pulse duration. In this paper, we present the extension of this

#176309 - $15.00 USD Received 18 Sep 2012; revised 2 Nov 2012; accepted 8 Nov 2012; published 14 Nov 2012

technique to 7-μJ energy levels by significant improvements in system and APPLN device designs. In section 2, we describe our OPCPA system and present our experimental results. In section 3 we describe the APPLN OPCPA devices, and in section 4 we provide details on the dispersion compensation scheme.

2. Experimental setup and results

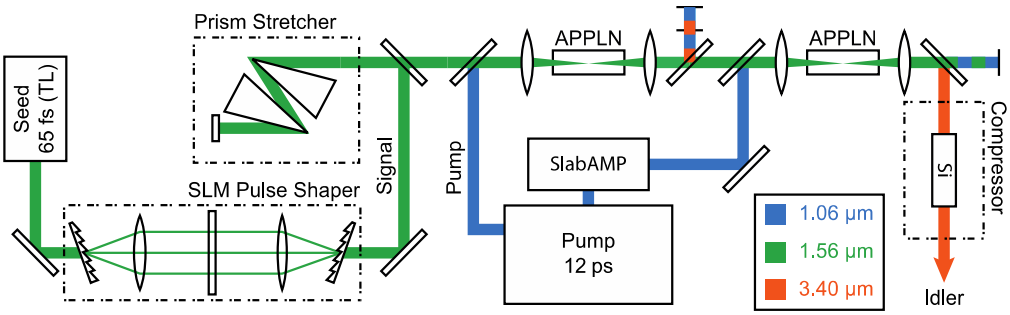

Fig. 1. Optical setup of the 2-stage OPCPA delivering 75-MW pulses. After the 2nd stage, the MIR idler is extracted and compressed to 75 fs duration by propagation through 150 mm bulk silicon (90% transmission). The spectral phase of the idler can be controlled by the pulse-shaper placed in the seed beam. During the OPA process, the spectral phase of the NIR seed is transferred to the MIR idler.

Our experimental setup is shown in Fig. 1. Compared to our previous MIR source [19], we changed the seed concept [35], integrated a home-built pump laser [25] into the OPCPA, and improved the APPLN devices [36]. The amplification system consists of a pre-amplifier (denoted OPA1) and a power amplifier (denoted OPA2). With the modified seed approach, we seed OPA1 with a near-infrared (NIR) signal, and seed OPA2 with the amplified signal output of OPA1. The generated MIR idler of OPA2 is then kept and sent into the pulse compressor. In our previous system, MIR seed pulses were generated from low-energy input pulses through difference frequency generation in a fan-out QPM grating [35]. In our new system, a commercial 1.56-μm femtosecond laser is used directly as the NIR seed to OPA1, corresponding to a significant reduction in system complexity.

The most significant advantage of this NIR seeding approach is efficiency: we found a material combination which allowed for bulk compression of the MIR pulses (with 90% transmission efficiency) while still compensating for second- and third-order dispersion of the stretched pulses. This efficiency is twice that of our previous prism-based compressor design [19]. Another significant benefit of the new seed concept is that the only elements that must be placed in the output MIR idler are a collimation lens and the bulk Si compressor. All other optical components in the amplifier path are optimized and aligned at the more standard and easier to detect 1 μm pump and 1.5 μm seed wavelengths, which allows for more precise and efficient alignment of the system.

In addition, at the telecommunication seed wavelength, many well-developed optical components are available. For example, we use a spatial light modulator (SLM) for high repetition rate pulse shaping. The use of such standard components is consistent with the overall design goal for the system: We aim at developing a reliable system that is useful for strong-field physics experiments on a daily basis. The NIR seeding approach is enabled by the collinear APPLN OPCPA geometry: since both the signal and idler pulses are collinear with the pump, they are usable for subsequent experiments or amplification. In contrast, in a non-collinear configuration, a useable idler (generated wave) can only be obtained by non-trivial compensation of its spatial chirp.

The pump source for OPA1 is a turn-key industrial laser (Time-Bandwidth Products Inc., Duetto) which operates at 1.064 μm and delivers 12-ps pulses at a repetition rate of 100 kHz, with an average output power of up to 11 W. Up to 8 W of this laser is used for OPA1, while

#176309 - $15.00 USD Received 18 Sep 2012; revised 2 Nov 2012; accepted 8 Nov 2012; published 14 Nov 2012

the remaining power is sent into a home-built Nd:YVO_4 slab amplifier to generate the pump pulses for OPA2 [25]. This slab amplifier yields a maximum power of up to 46 W (466 µJ at 12 ps pulse duration when operating at 100 kHz).

The pulse train of the pump laser oscillator is electronically stabilized to that of the seed laser with a phase locked loop (PLL). Our locking scheme yields a residual timing jitter of less than 150 fs rms, which is very small compared to the pump and stretched seed pulse durations. By setting the phase of the PLL we can control the delay between the pulses of the two oscillators by up to ± 1 ns. This approach allows us to control the overlap of seed and pump without any moving mechanical parts.

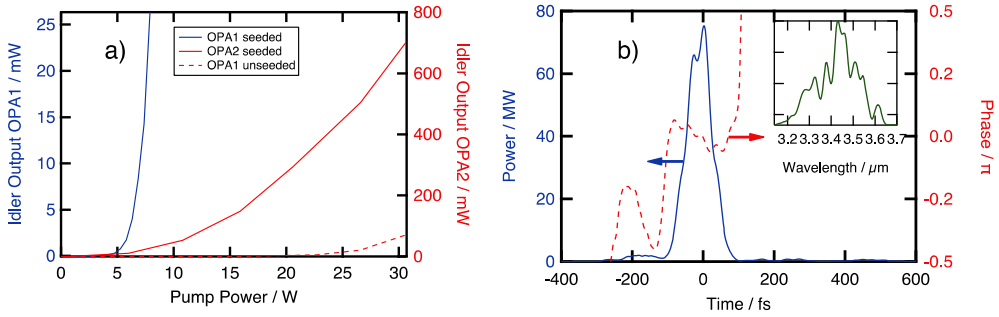

Fig. 2. (a) Pump-power dependence of OPA1 and OPA2. The maximum measured idler power after OPA1 is 26 mW (solid blue line), and there is no measurable OPG output (10 µW measurement threshold). The maximum idler power after both OPA2 and the bulk-compression stage is 700 mW, corresponding to 7 µJ (solid red line). We obtained an (over-)estimate of 72 mW for the optical parametric generation (OPG) background by blocking the seed pulses (dashed red line). This measurement is discussed further in section 3. (b) Reconstructed temporal pulse profiles from SHG-FROG after compression with 150-mm of bulk silicon. The inset shows the corresponding spectrum.

Before OPA1, the 1.56-µm seed pulses from the femtosecond fiber laser are stretched to approximately 2.6 ps by a two-prism silicon stretcher and a SLM-based pulse shaper. The holographic gratings used in this pulse shaper have a groove density of 600/mm; the dispersed pulses are collimated by an 800-mm cylindrical lens before passing through the SLM shown in Fig. 1. The energy of the stretched pulses reaching OPA1, after both the pulse shaper and the prism stretcher, is 87 pJ.

To support the required broadband output (as well as future bandwidth scaling) we use apodized, aperiodically poled MgO:$LiNbO_3$ for both OPA1 and OPA2. The QPM grating design is discussed in section 3. The pump and seed beams are collinearly overlapped in both amplification stages, with peak pump intensities of 6.8 GW/cm^2 (1/e^2 radius w = 250 µm) and 9.4 GW/cm^2 (w = 400 µm) in OPA1 and OPA2, respectively. The output idler power of the OPAs as a function of incident pump power is depicted in Fig. 2(a) (solid lines). The OPA2 curve was measured after collimation and compression, and hence shows that a final output pulse energy of 7 µJ is achieved. We characterized the output pulses using second harmonic generation (SHG) frequency resolved optical gating (FROG) [37]. The FROG-reconstructed temporal profile of the output pulses is depicted in Fig. 2(b), showing a pulse duration of 75-fs; this duration appears to be seed-limited. The corresponding power spectrum is shown as a function of wavelength in the inset.

3. Apodized APPLN amplifiers

In both amplifier stages we use 10-mm-long, 1-mm-wide, uncoated APPLN chips. The QPM chirp rate is given by $\kappa' = -dK_g/dz$, where $K_g(z)$ is the local grating k-vector. A chirp rate of $\kappa' = -2.5$ mm^{-2} is used to achieve a broad phase-matching spectral window ranging from 2.71 to 4.24 µm. The negative chirp rate was chosen since it yielded a higher beam quality than a

#176309 - $15.00 USD Received 18 Sep 2012; revised 2 Nov 2012; accepted 8 Nov 2012; published 14 Nov 2012

positive chirp. The sign of the chirp rate can play a role in effective lensing effects which occur during the parametric frequency conversion process [38]. These and other relevant effects will be discussed in more detail in future work. Another important property of the chip is the apodization. To avoid accumulation of spectral phase ripples or other high-order phase contributions during the amplification process, the nonlinear coupling is turned on and off adiabatically (smoothly and sufficiently slowly) at the input and output ends of the QPM grating [39]. The apodization is realized by rapidly varying the poling period (poling period apodization), resulting in dephasing of the three-wave mixing process (effectively reducing the nonlinear coupling). The grating profile is depicted in Fig. 3.

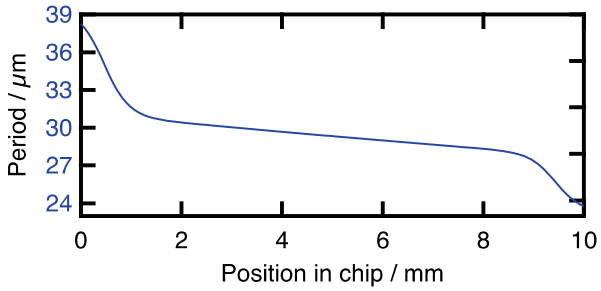

Fig. 3. Poling structure for the APPLN OPA devices used in both stages. An apodized linearly chirped QPM grating is used to ensure a smooth gain spectrum. The linear chirp rate is $\kappa' = -2.5\ \mathrm{mm}^{-2}$. The nonlinear coupling is turned on and off adiabatically at both ends, over a distance ~10% of the total length of the grating, by rapidly varying the poling period (increasing the magnitude of the chirp rate). The nominal QPM duty cycle is 50%.

With these apodized gratings, we obtain clean temporal pulse profiles after the bulk compressor, with almost all the pulse energy in the main pulse. Before designing this high-power, few-cycle OPCPA, we studied the effect of apodization on the pulse structure [36]. Without apodization the temporal structure breaks up into multiple sub-pulses, reducing peak intensity.

The focusing geometry is an important parameter of the OPCPA system design. APPLN OPAs can be affected by non-collinear gain guided modes [33]. If these modes exist, they can be amplified throughout the whole crystal, in contrast to collinear signal beams which experience gain only in the vicinity of its perfect phase-matching point [31]. Such gain guided modes are seeded by quantum noise and can therefore result in an increased optical parametric generation (OPG) background. With sufficient pump peak power that a large spot size with adequate intensity to support the collinear gain can be obtained, this gain guiding process can be suppressed at a given peak intensity, since the noncollinear beam components are dephased before they leave the large pump beam [33]. This high peak power is now available from our upgraded pump source. In the range of available pump powers we do not see a significant background from OPG. We estimated an upper limit for the OPG by blocking the seed before OPA1. The remaining output power of OPA1 is below the measurement threshold of 10 μW. When directed into OPA2, this small amount of OPG is amplified to 72 mW at full pump power of 30 W [red dashed line in Fig. 2(a)]. In the seeded case, we expect this small remaining background to be decreased substantially as a result of pump depletion.

4. Dispersion compensation

After amplification the pulses must be compressed in time. We designed the NIR pulse stretcher such that MIR pulse compression could be performed in a bulk crystal, thereby keeping the MIR losses as low as possible. During the OPA process, the spectral phase of the signal is transferred to the idler. Because both the phase and frequency shift of spectral components of the generated idler wave are inverted with respect to the signal seed wave, the

#176309 - $15.00 USD Received 18 Sep 2012; revised 2 Nov 2012; accepted 8 Nov 2012; published 14 Nov 2012

sign of the group delay dispersion (GDD) is reversed, but the sign of the third order dispersion (TOD) is maintained. Note that there are also additional contributions to the GDD and TOD of the generated idler wave due to the use of chirped QPM gratings, as discussed in [32].

Our stretching system for the 1.56-μm seed yields positive GDD and negative TOD. The 3.4-μm idler is generated with a negative GDD which is then compensated by the positive GDD of the bulk Si compressor placed after the OPCPA output. Two pieces of antireflection-coated bulk Si with a combined length of 150 mm are used. We were able to compress the 3.4-μm-pulses to 80 fs duration with a total transmission of 90% by using this seed stretching and Si bulk compressor combination.

To enable additional fine control of the dispersion, we placed a SLM-based pulse shaper in the seed beam path [40]. We used this shaper to pre-compensate the residual TOD on the idler, resulting in the seed-limited pulse duration of 75 fs shown in Fig. 2(b). More generally, with such a pulse shaper we can deliver the shortest possible pulses to an experimental target by pre-compensating for material dispersion occurring along the propagation to each specific experiment (vacuum chamber entrance windows, etc.). This approach therefore simplifies the operation of the laser for various applications.

5. Conclusion

In conclusion, we have demonstrated an OPCPA system for few-cycle pulse generation in the mid-infrared. The concept of seeding the OPCPA with the signal at 1.56 μm allows us to use standard optical components up to the 3.4 μm-idler extraction occurring after the final OPA stage. This design choice makes bulk compression with 90% efficiency possible. We achieve 75 fs pulse duration (<7 optical cycles) at 7 μJ output energy, corresponding to 700 mW of average power at a repetition rate of 100 kHz. To verify the usefulness of this source for strong-field experiments, we focused the 3.4-μm, 75 MW beam with an aspherical lens (EFL = 4 mm) into a gas target at ~100 mbar. Successful ionization of Xe, Ne and He confirms focusability to intensities $>10^{14}$ W/cm^2.

To our knowledge, this system is the first practical implementation of an OPCPA that uses apodized APPLN for the generation of clean, high-energy few-cycle pulses. By upgrading our pump source we have shown the energy scalability of the technique. In the next step we will replace our seed source in order to obtain broader bandwidths. With APPLN OPCPA devices, it should be possible significantly increase the bandwidth. With realistic improvements to the system, we therefore expect to generate few-cycle pulses with even higher energies.

Acknowledgments

This research was supported by the Swiss National Science Foundation through grant #200021_132504/1 and by the U.S. Air Force Office of Scientific Research (AFOSR) under grants FA9550-09-1-0233 and FA9550-05-1-0180.

#176309 - $15.00 USD Received 18 Sep 2012; revised 2 Nov 2012; accepted 8 Nov 2012; published 14 Nov 2012